Arabian Journal of Chemistry (2016) 9, 269–273

King Saud University

Arabian Journal of Chemistry

www.ksu.edu.sa
www.sciencedirect.com

ORIGINAL ARTICLE

Fabrication and characterization of mesoporous silica nanochannels inside the channels of anodic alumina membrane

Moataz M. Mekawy

Center of Materials Science, Zewail City of Science and Technology, Sheikh Zayed District, 12588, 6th of October City, Giza, Egypt

Received 1 April 2015; accepted 8 May 2015
Available online 21 May 2015

KEYWORDS

Mesoporous silica;
Anodic alumina membrane;
Nanochannels

Abstract Brij type surfactants (C_nEO_x) that have different chemical structures were used to fabricate 3D Mesoporous Silica Nanochannels (MSN) inside the channels of Anodic Alumina Membrane (AAM) under acidic conditions. The fabricated 3D MSN were characterized using TEM-ED, SEM, Small angle XRD, and N_2 isotherm. Results revealed that the synthesis of ordered 3D cubic *Im3m* mesostructures can be formed with tunable pore diameters varied from 4.0 to 4.9 nm that are partially affected with the length of ethylene oxide (EO) group in the template surfactant.

1. Introduction

Mesoporous silica materials including powders, monoliths, and films have received remarkable attention in the past two decades (Kresge et al., 1992; Lu et al., 2000; Zhao et al., 1998; El-Safty et al., 2005; Balaji et al., 2006). Their unique uniform pores ranging from a few to tens nm in diameter and stability in organic and inorganic solution phases could shed light on a plethora of different promising applications such as size-exclusive separation (Yamaguchi et al., 2004; El-Safty et al., 2010; Mekawy, 2011), enzymatic nanoreactors (Fu et al., 2008 Mekawy et al., 2011), sensors (El-Safty et al., 2008a,b) and nanofluidic devices (Yamashita et al., 2007).

Recently, synthesis of mesoporous silica inside the columnar channels of an anodic alumina membrane (AAM) has been extensively studied, and 1D or 2D hexagonally ordered or stacked (circular) mesostructure has been fabricated inside the columnar AAM channels by using cationic, nonionic and block copolymer surfactants as template and structural-guided synthesis (Martin, 1994; Yamaguchi et al., 2008; Nishizawa et al., 1995; Wu et al., 2004a,b; Platschek et al., 2006; Hu et al., 2014). However, the extensive synthesis conditions might lead to very difficult control over the 3D channel geometry in the final replica along the entire AAM channels. The key factor behind the control synthesis of 3D mesoporous channel geometry inside the AAM channels is to enhance the functionality of the membrane for future applications.

Syntheses of mesoporous silica materials with controlled morphology and tunable pore diameters have been previously reported using two different aspects: the direct mesoscopic

---

E-mail address: mmekawy@zewailcity.edu.eg

Peer review under responsibility of King Saud University.

Production and hosting by Elsevier

http://dx.doi.org/10.1016/j.arabjc.2015.05.007

self-assembly of surfactant and silica sol in an acidic solution (Huo et al., 1997; Che et al., 2004; Wang et al., 2003 and Wang et al., 2004; Marlow et al., 2000; Kleitz et al., 2001) and, the confinement evaporation-induced mesoscopic self assembly of surfactant and silica precursors within a porous nanochannel substrate (Lu et al., 2004; Yang et al., 2003; Yao et al., 2004; Wang et al., 2005; Chae et al., 2004; Wu et al., 2004a,b). In both schemes, by controlling the starting composition between the silica source and template surfactant, acidity, aging time and temperature, the morphology and the fabricated mesostructures could be controlled with nanochannels that have parallel or circular alignment to the porous substrate. The structural properties of parallel nanochannels which are responsible for the diffusion and mass transport mechanism could be used for numerous applications either as-made or grafted by cationic, anionic, hydrophilic or hydrophobic functional groups. Hence, the localized internal atmosphere inside the nanochannels could control the diffusion and mass transport mechanisms and thus, can be used for selective separation sciences, sensing and catalysis. Moreover, understanding and prediction of the mechanism of interaction which is responsible for the diffusion, extraction and mass transport within the nanochannels (Yamaguchi et al., 2006 and Yamaguchi and Teramae, 2008) could help achieving many successful applications of confined mesoporous silica membranes such as; diffusion of biomolecules (Gargiulo et al., 2013), adsorption of organic pollutants (El-Safty et al., 2012), biosensors (Itoh et al., 2014; Hotta et al., 2012; Fan et al., 2014), gas sorption (Chalal et al., 2015) and anion detection at the liquid/liquid interface (Gao et al., 2015).

Fabrication of hybrid mesoporous membranes, with pore diameters ranging from a few nm to tens of nm with different geometrical structures remains a challenge and very important research topic because they are considered as essential criteria for possible applications such as size and charge exclusive separation. In the past, various supporting membranes have been used as supports to regulate the synthesis of well ordered mesoporous silica materials within their ordered and uniform channels such as Polyurethane (Lin et al., 2008), Nafion (Álvarez and Fuertes, 2007) and Anodic Alumina Membranes (Martin, 1996, 1997). AAM showed superiority in being used on a large scale due to its availability, low cost, and low permeation resistance. Previous studies provided strong support for pursuing organized and uniform mesoporous silica membranes (Xomertakis et al., 2007 and Tian et al., 2003; Meoto and Coppens, 2014). Yet, recent progresses could be utilized to modify the synthesis protocols for more morphological control and better future applicability. Thus; fabrication of intrawire nanoporous structure with its lamellar disks perpendicular to the mesoporous silica wire axis (Hu et al., 2014), synthesis of silica nanotubes with orientation controlled mesopores (Zhang et al., 2012) and synthesis of polymers, metal oxides, and alloys magnetic nanoparticles coordinated with mesoporous silica membranes (Cauda et al., 2012 and Alamri et al., 2014) could be achieved.

The surfactant templated method has been extensively studied to fabricate different types of mesostructures. In this study, we report a synthesis pathway of 3D cubic *Im3m* MSN that are formed inside AAM pocket-like channels by using four different Brij type template surfactants which are alkyl-poly ethylene oxide surfactants (C_nEO_x) where n is the number of carbon atoms in the Lipophilic alkyl chain and x is the number of the hydrophilic ethylene oxide (EO) group.

2. Experimental procedure

2.1. Materials

Tetraethylorthosilicate (TEOS), was used as the silica source, ethanol and 0.1 M HCl were obtained from Wako Pure Chemical Industries, Ltd., Japan. The n-alkyl-oligo(ethylene oxide) surfactants, polyoxyethylene(10)cetyl ether (Brij 56, $C_{16}H_{33}(OCH_2CH_2)_{10}OH$, polyoxyethylene(20)cetyl ether (Brij 58, $C_{16}H_{33}(OCH_2CH_2)_{20}OH$, and polyoxyethylene(10)-stearyl ether (Brij 76, $C_{18}H_{37}(OCH_2CH_2)_{10}OH$, polyoxyethylene(20)stearyl ether and (Brij 78, $C_{18}H_{37}(OCH_2CH_2)_{20}OH$) were from Aldrich. Anodic Alumina Membrane (AAM) of 200 nm bulk pore size, 4.7 cm membrane diameter, and 60 μm thickness was from Whatman, UK. All materials were used as received without any further purification.

2.2. Synthesis and characterization

Our synthesis method consisted of two consecutive steps. First, a precursor solution was formed where the Brij surfactant was allowed to dissolve in ethanol under acidic conditions using HCl. After complete dissolution, TEOS was carefully added to the Brij solution. The starting reactant molar composition was 0.025: 2.52×10^{-3}: 0.22: 0.037 for TEOS: Brij surfactant: EtOH: HCl, respectively. The last mixture was refluxed for 2.5 h at 45 °C to give a precursor solution. In the second step, the precursor solution was infiltrated within the pores of AAM under moderate aspiration to form a Brij MSN-hybrid membrane. This MSN-hybrid membrane was allowed to dry and then calcined using SNOL Muffle Furnace at a rate of 2 °C/min until it reached a temperature of 500 °C which was maintained for 90 min. Hybrid membranes were collected, allowed to cool down and then characterized using TEM-ED (JEOL 2100 F), SEM (HITACHI S-3400N), Small angle XRD (Bruker D8 Advance) and N_2 isotherm (BELSORP MIN-II).

3. Results and discussion

Morphology of the synthesized MSN was studied using SEM. Fig. 1 shows the SEM images of MSN that have been formed within the pore-channels of AAM. Formation was observed and confirmed after partial and complete etching of the alumina matrix of the AAM by 5% H_3PO_4 as shown in Fig. 1(B) and (C), respectively.

Fig. 2(A) shows the small angle XRD patterns of the calcined MSN-hybrid membranes. The well resolved peaks of small angle XRD patterns were consistent with a face centered cubic mesostructure of *Im3m* space group. This reflects the well ordering of the fabricated MSN. The patterns indicate the formation of cubic mesostructure of *Im3m* space group with a highly ordered structure. The high intensity peak (1 1 0) indicates a large unit cell dimension between 8.3 and 8.9 nm (see Table 1) suggesting the formation of large cage-like cubic *Im3m* mesostructure. The XRD patterns of MSN-hybrid

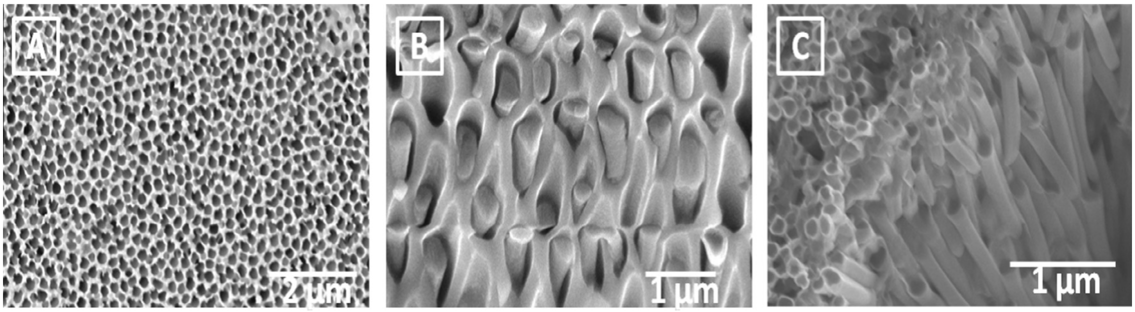

Figure 1 SEM of the AAM of 200 nm pore-channel diameter and 60 μm thickness without MSN (A), MSN inside the pore-channels of AAM after partial etching of alumina matrix with 5% H_3PO_4 for 30 min (B) and after complete etching of the alumina matrix with 5% H_3PO_4 for 420 min.

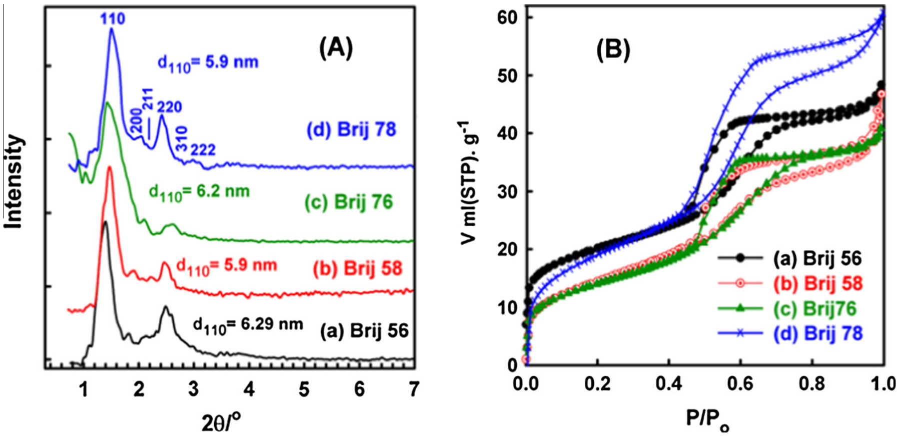

Figure 2 N_2 isotherms (A) and small angle XRD patterns (B) for MSN-hybrid membrane fabricated using Brij56, Brij58, Brij76, and Brij78, respectively.

Table 1 Textural parameters gained from small angle XRD and N_2 isotherm, pore diameter D (nm), unit cell a (nm), and BET surface area S_{BET} ($m^2\ g^{-1}$).

Surfactant	Chemical formula	D (nm)	a (nm)	S_{BET} ($m^2\ g^{-1}$)
Brij 56	$(C_{16}H_{33}(EO)_{10}OH$	4.0	8.9	66
Brij 58	$(C_{16}H_{33}(EO)_{20}OH$	4.5	8.4	65
Brij 76	$(C_{18}H_{37}(EO)_{10}OH$	4.3	8.8	62
Brij 78	$(C_{18}H_{37}(EO)_{20}OH$	4.9	8.3	66

membranes show evidence of a unique signal at low 2θ angle (<2°), which can be assigned to (1 1 0) diffraction, and presence of other well-resolved peaks in the range between $0.9° < 2\theta < 4.3°$, for the cubic crystallographic *Im*3*m* mesostructure. The intensity and resolution of all reflections strongly indicate a high ordering degree of the formed 3D architecture (El-Safty et al., 2008a,b).

Fig. 2(B) shows the N_2 isotherms of the calcined MSN-hybrid membranes. Isotherm results revealed that; the MSN-hybrid membranes show type IV isotherm with sharp inflection peaks of the adsorption/desorption branches. The adsorption isotherms exhibit well-defined hysteresis loop of H_2 and H_3 types according to IUPAC classification. The shape of each isotherm strongly indicates the formation of uniform mesoporous structures. In addition, there is a sharp increase in the adsorbed volume of N_2 due to capillary condensation occurring at a relative pressure p/p_o of ca. 0.50 with a high homogeneity in pore size distribution of the final product. The NLDFT based analysis shows narrow and well-ordered pore diameter distribution obtained from the absorption branch isotherm which indicates the formation of a uniform and homogeneous well ordered structure. The values of the average pore diameter of the adsorption branches are listed in Table 1.

Results also show that; the pore diameter increases as the length of the EO chain increases while having the same length of alkyl chain. In other words, the pore diameter could be remarkably affected with the length of EO group (Smarsly et al., 2001; Morishige and Kondou, 2012; Kipkemboi et al., 2009). This could be ascribed due to the partial embedding of EO group in the silica walls. Thus, the diameter can be controlled by the interface structure around the single EO chains within the silica framework. Moreover, the BET surface areas were found to be within the same range.

The HRTEM micrographs shown in Fig. 3 clearly revealed large domain sizes of ordered pore networks running along the 1D pore-channels of AAM membrane. The TEM images and their corresponding Fourier transform diffractograms (FTD) of cubic *Im3m* recorded along [1 0 0], and [1 1 1] indices indicate the formation of cubic *Im3m* organization with MSN for the

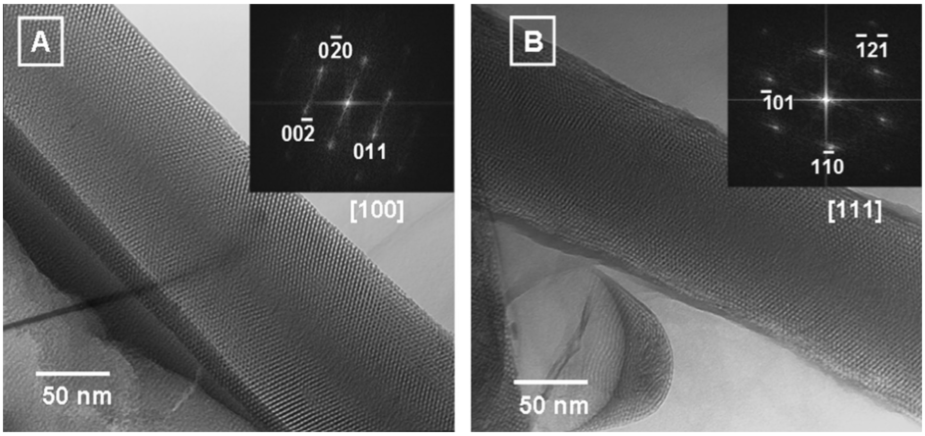

Figure 3 HRTEM images and FTD (inserts) patterns of the calcined MSN of 3D cubic *Im3m* (A, B) after etching of alumina hosts by the addition of 5% H_3PO_4 for 420 min at 25 °C. The TEM patterns of cubic *Im3m* were recorded along (A) [1 0 0] and (B) [1 1 1] zone axes.

first time using different Brij type surfactants, as consistent with the well-defined XRD patterns.

4. Conclusion

In summary, we have fabricated 3D mesoporous silica nanochannels inside the 1D pore-channels of AAM. The most prominent feature was the uniform mesoporosity and continuous ordering channels along all directions of the silica frameworks without distortion, indicating the integrity of the cubically ordered nanochannels. Moreover, the synthesis protocol and results show evidences for the fidelity of control design to form a free-standing alignment along the confinement channels, which is a promising feature of the fabricated hybrid membrane to permit a high flux and transport. Thus it can be promising for various future applications such as size-exclusive separation, catalysis, adsorption and sensors.

References

Alamri, H., Ballot, N., Long, J., Guari, Y., Larionova, J., Kleinke, K., Kleinke, H., Prouzet, E., 2014. Integrative synthesis of coordination polymers, metal oxides, and alloys magnetic nanoparticles in MSU mesoporous silica. Chem. Mater. 26, 875–885.

Álvarez, S., Fuertes, A.B., 2007. Synthesis of macro/mesoporous silica and carbon monoliths by using a commercial polyurethane foam as sacrificial template. Mater. Lett. 61, 2378–2381.

Balaji, T., El-Safty, S.A., Matsunaga, H., Hanaoka, T., Muzukami, F., 2006. Optical sensors based on nanostructured cage materials for the detection of toxic metal ions. Angew. Chem. Int. Ed. 45, 202.

Cauda, V., Torre, B., Falqui, A., Canavese, G., Stassi, S., Bein, T., Pizzi, M., 2012. Confinement in oriented mesopores induces piezoelectric behavior of polymeric nanowires. Chem. Mater. 24, 4215–4221.

Chae, W.-S., Lee, S.-W., Im, S.-J., Moon, S.-W., Zin, W.-C., Lee, J.-K., Kim, Y.-R., 2004. Templated carbon nanofiber with mesoporosity and semiconductivity. Chem. Commun., 2554.

Chalal, N., Bouhali, H., Hamaizi, H., Lebeau, B., Bengueddach, A., 2015. CO_2 sorption onto silica mesoporous materials made from nonionic surfactants. Microporous Mesoporous Mater. 210, 32–38.

Che, S., Liu, Z., Ohsuna, T., Sakamoto, K., Terasaki, O., Tatsumi, T., 2004. Synthesis and characterization of chiral mesoporous silica. Nature 429, 281.

El-Safty, S.A., Hanaoka, T., Mizukami, F., 2005. Large-scale design of cubic Ia3d mesoporous silica monoliths with high order, controlled pores, and hydrothermal stability. Adv. Mater. 17, 47.

El-Safty, S.A., Prabhakaran, D., Kiyozumi, Y., Mizukami, F., 2008a. Nanoscale membrane strips for benign sensing of hgii ions: a route to commercial waste treatments. Adv. Funct. Mater. 18, 1739.

El-Safty, S.A., Prabhakaran, D., Ismail, A.A., Matsunaga, H., Mizukami, F., 2008b. Three-dimensional wormhole and ordered mesostructures and their applicability as optically ion-sensitive probe templates. Chem. Mater. 20, 2644.

El-Safty, S.A., Mekawy, M.M., Yamaguchi, A., Shahat, A., Ogawa, K., Teramae, N., 2010. Organic–inorganic mesoporous silica nanostrands for ultrafine filtration of spherical nanoparticles. Chem. Commun. 46, 3917.

El-Safty, S.A., Shahat, A., Ismael, M., 2012. Mesoporous aluminosilica monoliths for the adsorptive removal of small organic pollutants. J. Hazard. Mater. 201–202, 23–32.

Fan, Y., Hotta, K., Yamaguchi, A., Ding, Y., He, Y., Teramae, N., Sun, S., Ma, H., 2014. Highly sensitive real-time detection of DNA hybridization by using nanoporous waveguide fluorescence spectroscopy. Appl. Phys. Lett. 105, 031103.

Fu, W., Yamaguchi, A., Kaneda, H., Teramae, N., 2008. Enzyme catalytic membrane based on surfactant- templated mesoporous silica formed within porous anodic alumina membrane. Chem. Commun. 7, 853.

Gao, K., Jiang, X.-H., Hu, D.-P., Bian, S.-J., Wang, M., Chen, Y., 2015. Impact of an ionic surfactant on the ion transfer behaviors at meso-liquid/liquid interface arrays. Chin. Chem. Lett. 26 (3), 285–288.

Gargiulo, N., De Santo, I., Causa, F., Caputo, D., Netti, P.A., 2013. Confined mesoporous silica membranes for albumin zero-order release. Microporous Mesoporous Mater. 167, 71–75.

Hotta, K., Yamaguchi, A., Teramae, N., 2012. Nanoporous waveguide sensor with optimized nanoarchitectures for highly sensitive label-free biosensing. ACS Nano 6, 1541–1547.

Hu, M.Z., Shi, D., Blom, D.A., 2014. Nanostructured mesoporous silica wires with intrawire lamellae via evaporation-induced self-assembly in space-confined channels. J. Nanomater., 8 Article ID 932160.

Huo, Q.S., Zhao, D.Y., Feng, J.L., Weston, K., Buratto, S.K., Stucky, G.D., Schacht, S., Schuth, F., 1997. Room temperature growth of mesoporous silica fibers: a new high-surface area optical waveguide. Adv. Mater. 9, 974.

Itoh, T., Shimomura, T., Hayashi, A., Yamaguchi, A., Teramae, N., Ono, M., Tsunoda, T., Mizukami, F., Stucky, G.D., Hanaoka, T.,

2014. Electrochemical enzymatic biosensor with long term stability using hybrid mesoporous membrane. Analyst 139, 4654–4660.

Kipkemboi, P.K., Kipronon, P.C., Ndalut, P.K., 2009. Preparation of porous silica materials via sol-gel nanocasting of nonionic surfactants: a mechanistic study on the self-aggregation of amphiphiles for the precise prediction of the mesopore size. Indian J. Chem. 48A, 498–503.

Kleitz, F., Marlow, F., Stucky, G.D., Schuth, F., 2001. Mesoporous silica fibers: synthesis, internal structure, and growth kinetics. Chem. Mater. 13, 3587.

Kresge, C.T., Leonowicz, M.E., Roth, W.J., Vartuli, J.C., Beck, J.S., 1992. Ordered mesoporous molecular sieves synthesized by a liquid-crystal template mechanism. Nature 359, 710.

Lin, Y., Li, H., Liu, C., Xing, W., Ji, X., 2008. Membranes with mesoporous SiO_2 layers via a facile dip-coating approach for direct methanol fuel cells. J. Power Sources 185, 904–908.

Lu, Y.F., Fan, H.Y., Doke, N., Loy, D.A., Assink, R.A., LaVan, D.A., Brinker, C.J., 2000. Evaporation induced self-assembly of hybrid bridged silsesquioxane film and particulate mesophases with integral organic functionality. J. Am. Chem. Soc. 122, 5258–5261.

Lu, Q., Gao, F., Komarneni, S., Mallouk, T.E., 2004. Ordered SBA-15 nanorod arrays inside a porous alumina membrane. J. Am. Chem. Soc. 126, 8650.

Marlow, F., Spliethoff, B., Tesche, B., Zhao, B., 2000. The internal architecture of mesoporous silica fibers. Adv. Mater. 12, 961.

Martin, C.R., 1994. Nanomaterials: a membrane-based synthetic approach. Science 266, 1961.

Martin, C.R., 1996. Membrane-based synthesis of nanomaterials. Chem. Mater. 8, 1739–1746.

Martin, C.R., 1997. A general template-based method for the preparation of nanomaterials. J. Mater. Chem. 7 (7), 1075–1087.

Mekawy, M.M., 2011. Fabrication of different silica nanotubes and examination of their catalytic activity in organic solvents. Res. Chem. Intermed. 37, 719.

Mekawy, M.M., Yamaguchi, A., El-Safty, S.A., Itoh, T., Teramae, N., 2011. Mesoporous silica hybrid membranes for precise size-1 exclusive separation of silver nanoparticles. J. Coll. Inter. Sci. 355, 348.

Meoto, S., Coppens, M.-O., 2014. Anodic alumina-templated synthesis of mesostructured silica membranes – current status and challenges. J. Mater. Chem. A 2, 5640.

Morishige, K., Kondou, Y., 2012. Formation and shrinkage of necks in microporous silica molecular sieve with ordered mesoporous structure. J. Phys. Chem. C 116, 3702–3706.

Nishizawa, M., Menon, V.P., Martin, C.R., 1995. Metal nanotubule membranes with electrochemically switchable ion-transport selectivity. Science 268, 700.

Platschek, B., Petkov, N., Bein, T., 2006. Tuning the structure and orientation of hexagonally ordered mesoporous channels in anodic alumina membrane hosts: a 2D small-angle X-ray scattering study. Angew. Chem. Int. Ed. 45, 1134.

Smarsly, B., Polarz, S., Antonietti, M., 2001. Preparation of porous silica materials via sol-gel nanocasting of nonionic surfactants: a mechanistic study on the self-aggregation of amphiphiles for the precise prediction of the mesopore size. J. Phys. Chem. B 105, 10473–10483.

Tian, Y.T., Meng, G.W., Gao1, T., Sun, S.H., Xie, T., Peng, X.S., Ye, C.H., Zhang, L.D., 2003. Alumina nanowire arrays standing on a porous anodic alumina membrane. Nanotechnology 15, 189–191.

Wang, J., Zhang, J., Asoo, B.Y., Stucky, G.D., 2003. Structure-selective synthesis of mesostructured/mesoporous silica nanofibers. J. Am. Chem. Soc. 125, 13966.

Wang, J., Tsung, C.-K., Hong, W., Wu, Y., Tang, J., Stucky, G.D., 2004. Synthesis of mesoporous silica nanofibers with controlled pore architectures. Chem. Mater. 16, 5169.

Wang, J., Tsung, C.-K., Hayward, R.C., Wu, Y., Stucky, G.D., 2005. Single-crystal mesoporous silica ribbons. Angew. Chem. Int. Ed. 44, 332.

Wu, Y., Cheng, G., Katsov, K., Sides, S.W., Wang, J., Tang, J., Fredrickson, G.H., Moskovits, M., Stucky, G.D., 2004a. Composite mesostructures by nanoconfinement. Nat. Mater. 3, 816.

Wu, Y., Livneh, T., Zhang, Y.X., Cheng, G., Wang, J., Tang, J., Moskovits, M., Stucky, G.D., 2004b. Templated synthesis of highly ordered mesostructured nanowires and nanowire arrays. Nano Lett. 4, 2337.

Xomertakis, G., Liu, N.G., Brinker, C.J., 2007. Anodic alumina supported dual-layer microporous silica. J. Membr. Sci. 287, 157.

Yamaguchi, A., Teramae, N., 2008. Fabrication and analytical applications of hybrid mesoporous membranes. Anal. Sci. 24, 25.

Yamaguchi, A., Uejo, F., Yoda, T., Yamashita, T., Uchida, T., Tanamura, Y., Teramae, N., 2004. Self-assembly of a silica–surfactant nanocomposite in a porous alumina membrane. Nat. Mater. 3, 337.

Yamaguchi, A., Watanabe, J., Mekawy, M.M., Fujiwara, R., Morita, K., Yamashita, T., Amino, Y., Chen, Y., Logudurai, R., Teramae, N., 2006. Extraction mechanisms of charged organic dye molecules into silica-surfactant nanochannels in a porous alumina membrane. Anal. Chim. Acta 556, 157–163.

Yamaguchi, A., Mekawy, M.M., Chen, Y., Suzuki, S., Morita, K., Teramae, N., 2008. Diffusion of metal complexes inside of silica-surfactant nanochannels within a porous alumina membrane. J. Phys. Chem. B 112 (7), 2024–2030.

Yamashita, T., Kodama, S., Ohto, M., Nakayama, E., Takayanagi, N., Kemmei, T., Yamaguchi, A., Teramae, N., Saito, Y., 2007. Use of porous anodic alumina membranes as a nanometre-diameter column for high performance liquid chromatography. Chem. Commun. 11, 1160.

Yang, Z., Niu, Z., Cao, X., Yang, Z., Lu, Y., Hu, Z., Han, C.C., 2003. Template synthesis of uniform 1D mesostructured silica materials and their arrays in anodic alumina membranes. Angew. Chem. Int. Ed. 42, 4201.

Yao, B., Fleming, D., Morris, M.A., Lawrence, S.E., 2004. Structural control of mesoporous silica nanowire arrays in porous alumina membranes. Chem. Mater. 16, 4851.

Zhang, A., Hou, K., Gu, L., Dai, C., Liu, M., Song, C., Guo, X., 2012. Synthesis of silica nanotubes with orientation controlled mesopores in porous membranes via interfacial growth. Chem. Mater. 24, 1005–1010.

Zhao, D., Huo, Q., Jianglin, F., Chmelka, B.F., Stucky, G.D., 1998. Continuous mesoporous silica films with highly ordered large pore structures. J. Am. Chem. Soc. 120, 6024.